Photoinduced Electron Transfer at Liquid/Liquid Interfaces. 1. Photocurrent Measurements Associated with Heterogeneous Quenching of Zinc Porphyrins

David J. Fermín, Zhifeng Ding, H. Dung Duong, Pierre-François Brevet, and Hubert H. Girault*

Laboratoire d'Electrochimie, Departement de Chimie, Ecole Polytechnique Fédérale de Lausanne, CH-1015 Lausanne, Switzerland

Received: July 28, 1998; In Final Form: October 8, 1998

Photocurrent responses associated with the heterogeneous quenching of water-soluble zinc tetrakis-(carboxyphenyl)porphyrin (ZnTPPC) by ferrocene and diferrocenylethane are studied at the water/1,2-dichloroethane interface. Basic features of the photocurrent transients are analyzed within the framework of classical photoinduced electron-transfer mechanisms. The potential dependence of the photocurrent at various light intensities and porphyrin concentrations provides a quantitative analysis of photoinduced heterogeneous electron-transfer kinetics at interfaces between two immiscible electrolyte solutions (ITIES). The dependence of the photocurrent intensity upon porphyrin concentration indicates that most of the photoresponses arise from sensitizer adsorbed at the liquid/liquid junction. The adsorption of porphyrins as well as the formation of interfacial ion pairs are confirmed by capacitance measurements. The rate of electron transfer was found to be of the same order as the lifetime of the excited state. The maximum quantum yield was estimated to be 60% for the photooxidation of ferrocene. The high surface charge introduced by the specific adsorption of nonprotonated ZnTPPC perturbs the potential distribution across the liquid/liquid interface. This phenomenon is reflected in the potential dependence of the surface coverage. The potential dependence of the electron-transfer rate constant is briefly discussed in terms of the existing models for ITIES. The possibility of novel solar energy conversion devices where the photoinduced electron transfer does not intimately involve a solid electrode is also envisaged.

1. Introduction

Interest in electron-transfer reactions (ET) at interfaces between two immiscible electrolyte solutions (ITIES) has been recently stimulated by novel experimental approaches.[1−9] Further excitement has been risen by claims of experimental evidence of the inverted Marcus region at the polarized water/benzene interface.[9] Photoinduced heterogeneous ET is a rather interesting approach to these type of reactions, where sensitizer and quencher are located in different liquid phases. Although very few reports have dealt with photochemistry at ITIES, extensive research in the homogeneous phase has led to the establishment of key concepts.[10] For instance, the general mechanism has been described in terms of the formation of an intermediate complex after the electron-transfer step, which is commonly called a geminate ion pair. This species can dissociate to yield the final products or undergo recombination regenerating the ground state. The factors controlling this competition largely depend on the charge and structure of both ions, as well as the properties of the solvent.[10,11] The presence of micelles and microemulsions has been proven to enhance the separation of geminate ion pairs on the basis of electrostatic forces and differences in hydrophilicity.[12] Steiner and Ulrich[13] have also reviewed the effects of magnetic fields in micellar cages, which provide further increments of the quantum yield.

At polarized ITIES, two types of processes can lead to photocurrent signals involving ET steps,[14] photoinduced electron transfer followed by ion transfer (PE-IT) and interfacial photoinduced electron transfer (IPET). Photocurrent responses associated with PE-IT processes have been studied by Kotov and Kuzmin.[15−17] In this case, the observed photocurrents correspond to the transfer across the liquid/liquid interface of the products generated in a homogeneous photoreaction. Photoresponses originating from the protoporphyrins/quinones and the quinones/tetraphenylborate systems were studied at the water/1,2-dichloroethane (DCE) interface. The differential equations involving the generation and transfer of the photoinduced products were solved in order to describe the time-dependent photocurrent.[16] On the other hand, photocurrent responses associated with IPET reactions are rather more difficult to study due to interferences arising from the transfer of either ionic reactants or products.

The pioneer works by Mauzerall and co-workers have described the dynamic of photoresponses between porphyrin species in phospholipid bilayer membranes and redox couples in aqueous solution.[18−22] Although these studies do not feature an ITIES, the nature of the electron-transfer step is heterogeneous and involves a nonsolid surface. Girault et al.[23,24] have studied the photoinduced electron transfer between $Ru(bpy)_3^{2+}$ in water and the quenchers C_7V^{2+} and TCNQ in DCE,

$$[Ru(bpy)_3]^{*2+}_{water} + [C_7V]^{2+}_{DCE} \rightarrow [Ru(bpy)_3]^{3+}_{water} + [C_7V]^{\bullet+}_{DCE} \quad (1)$$

$$[Ru(bpy)_3]^{*2+}_{water} + TCNQ_{DCE} \rightarrow [Ru(bpy)_3]^{3+}_{water} + TCNQ^{\bullet-}_{DCE} \quad (2)$$

In both processes, reactants and products are confined to each phase over a certain potential range, allowing the study of the photocurrent associated with the electron-transfer step. Marecek

10.1021/jp983196m CCC: $15.00
Published on Web 11/18/1998

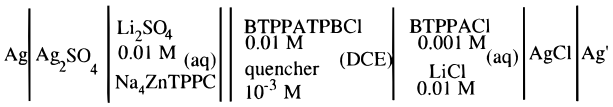

Figure 1. Representation of the electrochemical cell employed in all measurements. The porphyrin is dissolved in the aqueous phase containing Li_2SO_4.

et al.[25] have also reported IPET responses for $Ru(bpy)_3^{2+}$ in the organic phase (either DCE or benzonitrile) and methyl viologen in the aqueous phase. In these systems, however, the photocurrent signals were severely complicated by transfer of reactants and products. Other recent contributions have involved optical techniques such as second harmonic generation[26] and time-resolved fluorescence[27] and absorption[28] spectroscopies.

We have recently reported photocurrent transients associated with heterogeneous quenching of the water-soluble zinc tetrakis-(carboxyphenyl)porphyrin (ZnTPPC).[29] The sign of the photocurrent was reversed upon replacing an electron donor by an acceptor in the DCE phase. Furthermore, the transient responses were dependent on the applied potential, showing similar features to those observed at illuminated semiconductor/electrolyte junctions in the presence of electron−hole recombination. In the present paper, the dependence of the photocurrent on the applied potential, porphyrin concentration, and light intensity are considered. It is concluded that the porphyrin involved in the photoresponses is effectively adsorbed at the liquid/liquid junction.

2. Experimental Section

All electrolyte solutions were prepared from analytical grade reagents. The supporting electrolyte in the organic phase was bis(triphenylphosphoranylidene) ammonium tetrakis(4-chlorophenyl)borate (BTPPATPBCl). This salt was prepared by metathesis of BTPPACl and KTPBCl in a 2:1 mixture of methanol and water and was recrystallized in acetone. Aqueous solutions were prepared with purified water from a Milli-Q 185 system. All other reagents were used without further purification. The sodium salt of the porphyrin $ZnTPPC^{4-}$ was obtained from Porphyrin Products Inc.

The electrochemical cell is schematically displayed in Figure 1. For all experiments, the concentration of the quencher in the organic phase was in excess with respect to the porphyrin concentration. The Galvani potential difference across the liquid/liquid interface was estimated by taking the formal transfer potential of tetramethylammonium $\Delta_o^w\phi^{0'}_{TMA^+}$ as 0.160 V.[30]

Illumination was provided by a green He−Ne laser (543 nm). The incident light intensity was monitored simultaneously by a photomultiplier tube (PMT). The water/DCE junction (1.53 cm^2) was polarized via a custom-built four-electrode potentiostat. The all-glass cell contains two lateral compartments for the reference electrodes, which were approached to the interface by luggin capillaries. Under this arrangement, the reference electrodes were not under illumination, avoiding any photopotential interference.[23] Photocurrent measurements were also recorded under chopped illumination by a lock-in amplifier SR830 (Stanford Research). In these experiments, the output of the PMT was employed as the phase reference for the lock-in detection.

3. Results

A cyclic voltammogram of the water/DCE interface in the dark containing ZnTPPC and diferrocenylethane (DFcEt) is displayed in Figure 2. By convention, a positive current corresponds to the transfer of a positive charge from the aqueous to the organic phase. The voltammogram exhibits a potential window of nearly 500 mV in which no significant Faradaic responses are observed in the dark. The positive potential limit is determined by the transfer of Li^+ from water to DCE, while the negative limit is given by the transfer of SO_4^{2-} [30] and the porphyrin species. The absence of any Faradaic response within these limits indicate that no electron exchange occurs via the ground state of the sensitizer.

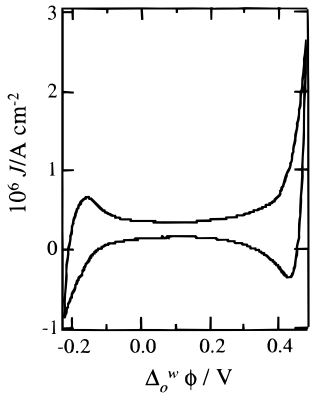

Figure 2. Cyclic voltammogram recorded at 0.01 V s^{-1} in the presence of 10^{-4} mol dm^{-3} $Na_4ZnTPPC$ and 10^{-3} mol dm^{-3} DFcEt in the aqueous and DCE phases, respectively.

Photocurrent transient responses for a porphyrin concentration of 10^{-4} mol dm^{-3} are displayed in Figure 3 at various Galvani potential differences. Photocurrent signals increase from effectively zero to steady-state values as high as 6×10^{-7} A cm^{-2} for a photon flux of 6.41×10^{15} cm^{-2} s^{-1}. The concentration of the quencher in DCE was 10^{-3} mol dm^{-3}. At potentials below 0.30 V, the on-transients exhibit positive in-phase responses followed by a decay to a steady-state value. During the off-transients, a negative overshoot is observed followed by a relaxation to zero. These responses resemble the characteristic transients at semiconductor/electrolyte junctions in the presence of interfacial recombination.[29,31] At potentials higher than 0.30V, the photocurrent exhibits a delay with respect to the signal arising from the PMT. At these potentials, it is observed that the photocurrent rising lags behind the light-on signal, while the decay is rather slow during the off-transient. The origin of these slow photocurrent transients is related to heterogeneous photoreactions with the organic supporting electrolyte BTPPATPBCl. Photocurrent transients in the absence of the ferrocene derivative at various potentials are also displayed in Figure 3 (dotted lines). At potentials more positive than 0.20 V, slow rising portions of the photocurrent are observed upon illumination. During the off-transients, the photocurrent also relaxes slowly to zero. Although the mechanism behind these type of responses is currently under investigation, it is expected that the anion $TPBCl^-$ is readily involved. Previous studies have shown that the oxidation potential of this anion under the same electrolyte conditions is 0.51 V with respect to the Fc/Fc^+ redox couple.[5] Recent preliminary studies indicate that by replacing $TPBCl^-$ by tetrakis(pentafluorophenyl)borate these photoresponses are substantially diminished. At potentials more negative than 0.20 V, negative photocurrents are also observed.

Photocurrent potential curves obtained in the presence of DFcEt under chopped illumination and lock-in detection are shown in Figure 4 at various illumination intensities. The photocurrents are directly proportional to the light intensity, suggesting that the diffusion of the excited state is negligible under the present experimental conditions. Several features can be highlighted from the in-phase (j_{photo}^{re}) and quadrature (j_{photo}^{im})

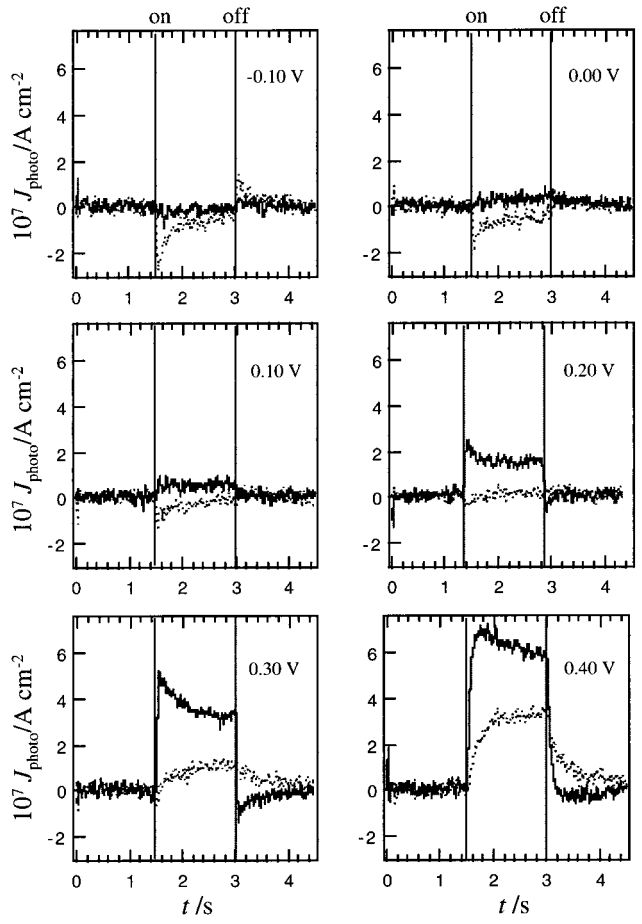

Figure 3. Photocurrent transient measurements in the presence (solid lines) and absence (dotted lines) of DFcEt at various Galvani potential differences. The concentration of the porphyrin was 10^{-4} mol dm^{-3}. The incident photon flux was 6.41×10^{15} cm^{-2} s^{-1}. No photoresponse was observed in the absence of porphyrin. Vertical lines correspond to the on−off signals recorded from the PMT simultaneously.

components of the photocurrent as a function of the Galvani potential difference. At potentials between −0.10 and 0.10 V, j_{photo}^{re} exhibits a small negative photocurrent which increases with the light intensity. In the same potential range, j_{photo}^{im} remains very small. As the potential is increased, the real component becomes positive and exhibits a maximum at about 0.35 V. The imaginary component also shows a maximum at 0.23 V, which is followed by a change of sign at 0.28 V and eventually a minimum at 0.40 V.

The various features observed in the photocurrent potential curves in Figure 4 are connected to the different relaxation modes of the transient responses (Figure 3). Although fundamental aspects of dynamic photoresponses associated with periodic light perturbations have been widely discussed,[31,32] some key points could be addressed. For instance, a back electron-transfer process introduces a photocurrent decay during the on-transient and a negative overshoot in the off-transient, generating a phase shift with respect to the light perturbation. This phase shift manifests itself as positive j_{photo}^{re} and j_{photo}^{im}. This is the behavior observed in Figures 3 and 4 in the potential range between 0.10 and 0.30 V. On the other hand, the slow increment of the photocurrent upon illumination and the slow decay to zero during the off-transient recorded at high potentials originate a negative quadrature component. This change in the shape of the transient responses coincides with the increase of the background photocurrent shown in Figure 3. An important parameter to be considered in this analysis is the chopping

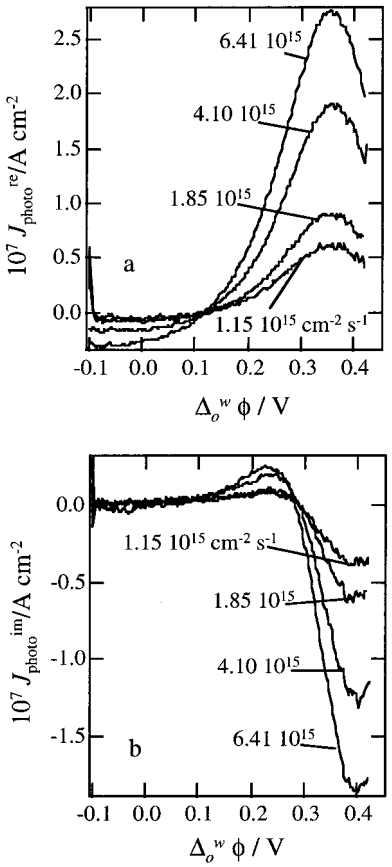

Figure 4. In-phase (a) and quadrature (b) components (of the photocurrent in the presence of DFcEt under chopped illumination at 12 Hz at various photon fluxes. The aqueous phase contains 10^{-4} mol dm^{-3} $Na_4ZnTPPC$. The imaginary part exhibits a positive signal associated with the recombination step and a negative signal in connection to the slow-rising responses at high potentials.

frequency. It is observed that the maximum of j_{photo}^{re} shifts to higher potentials as the frequency is decreased. Similarly, the positive region of j_{photo}^{im} is extended to higher potentials with decreasing frequencies. This behavior is consistent with the slow photoresponses at potentials close to 0.40 V. It should also be noticed that although the lock-in photocurrent appears in-phase close to 0.30 V ($j_{photo}^{im} = 0$) in Figure 4, recombination-like signals are still observed in the on−off transients of Figure 3. This is another effect linked to the chopping frequency. At 12 Hz, most of the recombination signals observed in the transient measurements appear to be frozen out, therefore only the in-phase component is detected.[31] An additional contribution to be considered is the RC constant of the cell, which lies in the range of 100 Hz or less. Experiments performed with IR compensation as well as with a smaller surface area (0.2 cm^2) did not show substantial differences within the same frequency range. These results indicate that although contributions from the RC constant are always present, these become more evident at higher frequencies or more positive potentials.

A rather interesting observation is related to the photocurrent dependence on the angle of illumination. The results shown in Figure 4 correspond to an incident light perpendicular to the interface. However, the photocurrent density remains practically unchanged under illumination in total internal reflection (TIR). At the water/DCE interface, TIR is achieved with illumination from the organic phase at an angle higher than 67°.[27] In TIR, the light penetration into the aqueous phase is limited to few hundreds of nanometers. The fact that the photocurrent depends linearly with light intensity but it is unaffected by the angle of

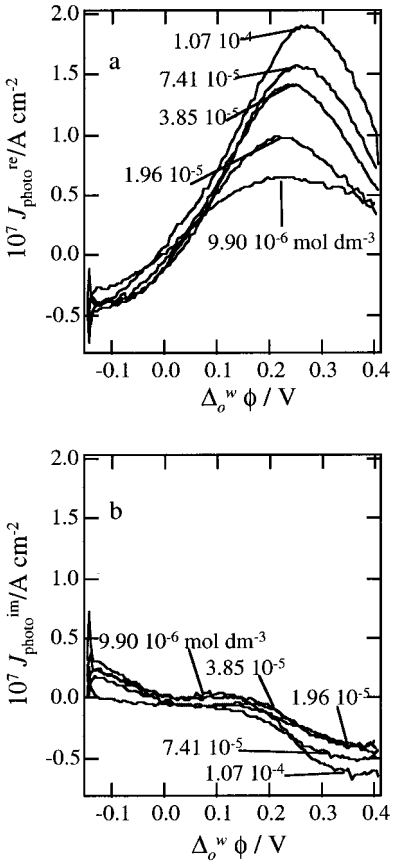

Figure 5. In-phase (a) and quadrature (b) components of the photocurrent in the presence of Fc at various porphyrin concentrations. The chopping frequency was 12 Hz, and the photon flux was 6.41×10^{15} cm^{-2} s^{-1}.

illumination suggests that the porphyrin involved in the electron-transfer step is mostly confined to the contact surface between both liquids.

The photocurrent dependence on the concentration of porphyrin in the aqueous phase is displayed in Figure 5. The quencher employed in these measurements was ferrocene (Fc). Comparisons between real (Figure 5a) and imaginary components (Figure 5b) indicate that recombination is effectively frozen out at the measuring frequency (12 Hz), simplifying considerably the forthcoming analysis. The overall photocurrent increases with increasing concentration of ZnTPPC; however, this dependence varies with the applied potential difference. At potentials close to 0.10 V, the photocurrent reaches a saturation at low porphyrin concentrations. At higher potentials, the photocurrent increases monotonically with the concentration of ZnTPPC. These results clearly indicate that not only is the photocurrent associated with adsorbed porphyrin at the interface but the surface coverage is also affected by the applied potential difference.

Further evidence of the porphyrin adsorption at the water/DCE interface is gathered from the potential dependence of the interfacial capacitance displayed in Figure 6. These curves were recorded at various concentrations of the porphyrin salt in the dark and in the absence of quenchers in the organic phase. The ac potential featured a frequency of 6 Hz and a 4 mV amplitude. The differential capacitance was calculated from the admittance employing an equivalent circuit composed of the uncompensated resistance R and the interfacial capacitance C_{int} in series. It can be observed that in the absence of porphyrin, the minimum of the capacitance is located at about 0.02 V. As the concentration of the sensitizer is increased, the minimum shifts toward positive

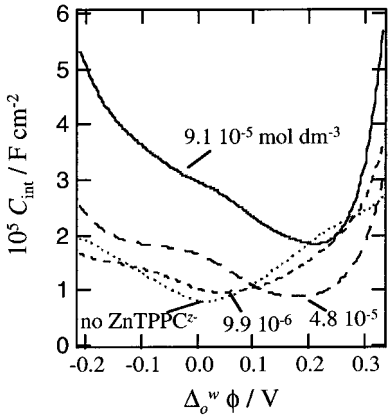

Figure 6. Differential capacitance potential curves at various porphyrin concentrations. The capacitance value was estimated from admittance curves recorded at 6 Hz and a 4 mV amplitude, assuming a RC series connection. A 0.20 V shift of the minimum upon adding a concentration of 4.8×10^{-5} mol dm^{-3} is observed. This shift is associated with the specific adsorption of porphyrin at the liquid/liquid contact surface. The increase of the differential capacitance toward negative potential suggests interfacial ion paring between porphyrin and the organic cation $BTPPA^+$.

potentials up to a value close to 0.22 V. At concentrations higher than 5×10^{-5} mol dm^{-3}, the position of the minimum becomes independent of the concentration but the overall capacitance increases. The shift of the potential of minimum capacitance indicates the presence of a surface excess charge associated with the specific adsorption of the $ZnTPPC^{4-}$.[33] Moreover, the strong increment of the capacitance at potentials less positive than 0.20 V suggests the formation of interfacial ion pairs between the porphyrin and $BTPPA^+$.[2,34] Toward negative potentials, the excess charge associated with ion pairing increases as the surface concentration of the organic cation is increased.

4. Discussion

4.1. On the Origin of the Photocurrent Responses. The photooxidation of a species Q located in the organic phase by a sensitizer S in the aqueous phase can be generally described by,

$$S_w \xrightarrow{h\nu} S_w^* \qquad \text{(photoexcitation)} \tag{3}$$

$$S_w^* \xrightarrow{k_d} S_w \qquad \text{(decay of the excited state)} \tag{4}$$

$$S_w^* + Q_o \xrightarrow{k_{et}} [S^- \cdots Q^+]_{int} \qquad \text{(electron transfer)} \tag{5}$$

$$[S^- \cdots Q^+]_{int} \xrightarrow{k_{ps}} S_w^- + Q_o^+ \qquad \text{(product separation)} \tag{6}$$

$$[S^- \cdots Q^+]_{int} \xrightarrow{k_{rec}} S_w + Q_o \qquad \text{(recombination)} \tag{7}$$

where $[S^- \cdots Q^+]_{int}$ is an intermediate species denominated photoinduced interfacial ion pair, in analogy to common photochemical terminology.[10] The subindexes w, o, and int stand for the aqueous, organic, and interfacial regions, respectively. At polarized interfaces, electron exchange reactions between S and Q are associated with Faradaic responses. By convention, the electron-transfer step (eq 5) and the recombination reaction (eq 7) exhibit a positive and a negative photocurrent, respectively. Both electron-transfer processes compete with parallel reactions. For instance, the excited state S_w^* can either be reduced by the quencher (eq 3) or decay to the ground state (eq

4). On the other hand, the photoinduced interfacial ion pair can undergo recombination or effectively dissociate (eq 6) yielding the final products. The dependence of each of these rate constants with the applied potential will determine the potential dependence of the photocurrent.

Most of the photocurrent potential features in the presence of electron donors in the organic phase can be described by the general mechanism of eqs 3−7. The positive j_{photo}^{im} observed in the range 0.15−0.30 V (Figure 4) is associated with the recombination current, which is determined by k_{ps} and k_{rec}. As mentioned previously, these phenomena are linked to the relaxation of the photocurrent following an illumination step and the negative overshoot in the off-transient (Figure 3). The increase of the overall photocurrent with increasing potentials indicates that k_{et} also increases in comparison to the rate constant of the excited-state decay, k_d. This potential dependence is reversed upon replacing the ferrocene derivative by an electron acceptor such as TCNQ.[29] In this case, the photocurrent exhibits a negative sign and increases as the applied potential difference is shifted to negative values. Additionally, the role of the interfacial chemistry of sensitizers and quenchers is a fundamental parameter in the photocurrent dynamics. For instance, comparisons between Figures 4 and 5 show that the photocurrent is slightly higher for DFcEt, while recombination appears slower in the presence of Fc. However, estimations of the redox potentials of both species employing a Pt microelectrode in the DCE phase provide very close values, i.e., $E_{DFcET^+/DFcET} = -0.088$ V and $E_{DFcET^{2+}/DFcET^+} = 0.070$ V with respect to $E_{Fc^+/Fc}$. Furthermore, taking the redox potential of ferrocene in DCE with respect to SHE as $E_{Fc^+/Fc} = 0.406$ V,[35] a potential difference of ca. 0.780 V is estimated against the oxidation potential of the $ZnTPPC^{4-}$ triplet state.[36]

The mechanism given by eqs 3−7 is only valid in the potential range where the photocurrent associated with the organic supporting electrolyte is negligible. In Figure 3, it is observed that the contribution of the photoprocess involving BTPPATPBCl becomes more evident at potentials close to the edges of the window. This rather interesting result suggests that photocurrent involving ionic quenchers may increase not only due to the increase of k_{et} but also by increasing the interfacial concentration of the reactants. We shall come back to this point after discussing the potential dependence of the photocurrent conversion efficiency.

4.2. Photocurrent Dependence on the Porphyrin Concentration. According to eqs 3−5, the surface density of the excited state (Γ_s^*) is determined by the photon flux to the interface (I_0) and the rate constants of electron transfer (k_{et}) and decay of the excited state (k_d).

$$d\Gamma_s^*/dt = I_0\sigma\Gamma_s - (k_{et} + k_d)\Gamma_s^* \tag{8}$$

where σ is the optical capture cross section of the porphyrin at the wavelength of illumination (543 nm) and Γ_s is the surface density of the ground-state sensitizer. k_{et} is taken as a pseudo-first-order rate constant (s^{-1}), considering that the surface concentration of the quencher is in excess. When it is assumed that Γ_s is constant, the steady-state concentration of the excited state is simply given by

$$\Gamma_s^* = \frac{I_0\sigma}{(k_{et} + k_d)}\Gamma_s \tag{9}$$

In the absence of recombination processes, it follows that the steady-state photocurrent density (j_{photo}) corresponds to

$$j_{photo} = ek_{et}\Gamma_s^* = ek_{et}\frac{I_0\sigma}{(k_{et} + k_d)}\Gamma_s \tag{10}$$

Equation 10 establishes a linear dependence of the photocurrent with the photon flux. In Figure 4, it is observed that the photocurrent increases linearly with the photon flux, indicating that Γ_s is constant at these illumination levels. The fact that the surface concentration of porphyrin is effectively constant suggests that diffusion effects are negligible. At photocurrent densities above 10^{-6} A cm^{-2}, diffusion processes become more evident. From the results displayed in Figure 5, the photocurrent signal is determined by the adsorbed porphyrin at the liquid/liquid junction. Assuming a Langmuir isotherm, eq 10 can be rewritten as

$$j_{photo} = ek_{et}\frac{I_0\sigma}{k_{et} + k_d}\left[\frac{\beta c_b}{1 + \beta c_b}\right]N_s \tag{11}$$

where N_s is the maximum surface density and c_b is the bulk concentration of ground-state porphyrin. β is the Langmuir isotherm parameter. The total photocurrent as a function of the ZnTPPC concentration is displayed in Figure 7 at various potentials. This figure is constructed from the data shown in Figure 5. The line fittings were estimated from eq 11, taking σ as 10^{-17} cm^2 and N_s as 5 10^{-13} cm^{-2}. Flash photolysis measurements in TIR and in the presence of oxygen provided a value for k_d of 10^5 s^{-1}. Two adjusting parameters were employed, k_{et} and β. The potential dependence of k_{et} will be discussed in the next section. From Figure 7, it is observed that the photocurrent becomes less dependent on c_b with increasing porphyrin concentration. A rather interesting point is that, within the same concentration range, the photocurrent is close to saturation at 0.10 V, while at 0.30 V, it still shows a strong dependence on c_b.

The surface coverage of porphyrin (θ) was estimated from the parameter β. The dependence of θ on the applied Galvani potential difference is shown in Figure 8. In Figure 8a, it is observed that the porphyrin coverage decreases from nearly unity to less than 0.7 as the potential is increased from 0.10 to 0.40 V. This behavior reflects a potential-induced desorption of a negatively charged porphyrin species as the potential in the bulk aqueous phase becomes more positive. Potential-induced adsorption−desorption has been reported by Higgins and Corn[37] for the surfactant 2-(*n*-octadecylamino)naphthalene-6-sulfonate at the water/DCE interface. Assuming a Langmuir isotherm, the potential dependence of θ can be generally expressed in terms of

$$\ln\left(\frac{\theta}{1-\theta}\right) = \ln\left(\frac{a_{ZnTPPC^{z-}}}{a_{H_2O}}\right) - \frac{\Delta G^\circ}{RT} + \frac{zbF}{RT}\Delta_o^w\phi \tag{12}$$

where the first term involves the ratio of the porphyrin and water activities, ΔG°, is the Gibbs energy of adsorption and b is the fraction of the Galvani potential difference in the aqueous side. Figure 8b shows that the logarithm of the ratio $\theta/(1-\theta)$ is linearly dependent on the applied Galvani potential difference. Deviation of this linear behavior is observed at high $\Delta_o^w\phi$ where the potential distribution across the interface could be disturbed by transfer of the supporting electrolyte. From the representation in Figure 8b and eq 12, ΔG° was estimated to be of the order of −41 kJ mol^{-1}, indicating the strong specific adsorption of the porphyrin at the interface. Assuming that the net charge of the adsorbed species is $z = -4$, it follows from the slope in Figure 8b that $b = 0.05 \pm 0.01$. The value of b

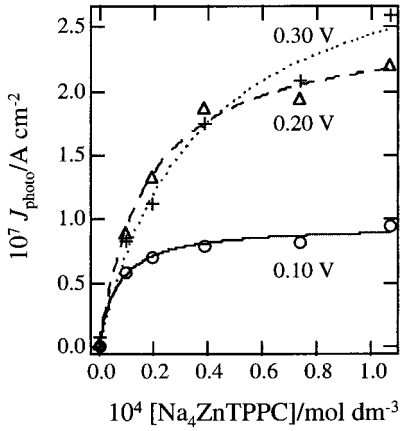

Figure 7. Total photocurrent as a function of the porphyrin concentration at various potentials. Experimental points were obtained from Figure 5. Fitting lines correspond to eq 11, assuming σ as 10^{-17} cm^2, N_s as 5×10^{13} cm^{-2}, and k_d as 10^5 s^{-1}.

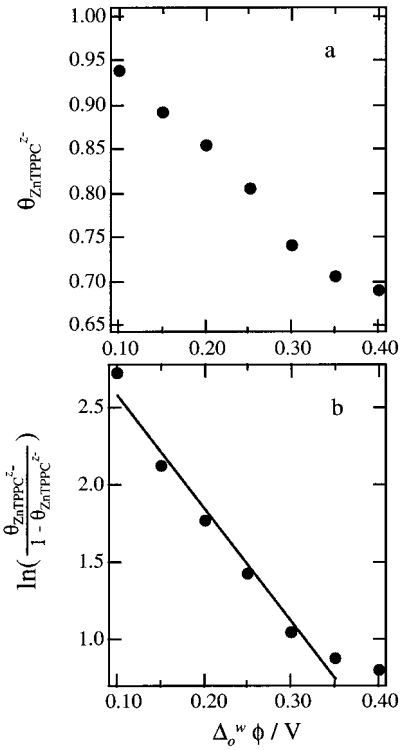

Figure 8. (a) Porphyrin coverage as a function of the Galvani potential difference. (b) Plot of $\ln(\theta/(1-\theta))$ as a function of the Galvani potential difference. The linear correlation indicates a Langmuir behavior of the adsorbed porphyrin.

suggests that approximately 5% of the applied Galvani potential difference occurred in the aqueous phase. This rather low ratio indicates that the potential distribution across the interface is strongly affected by the presence of charged porphyrin species. Specific adsorption and the formation of an interfacial ion pair with the organic cation $BTTPA^+$ could be responsible for an increase of the interfacial charge at the aqueous side, decreasing the potential drop in this region.

4.3. Potential Dependence of the Electron-Transfer Rate Constant k_{et}. The dependence of k_{et} on the applied Galvani potential difference is shown in Figure 9. These data were obtained from the fits described in Figure 7. It is observed that k_{et} increases as the potential increases, showing a maximum value at 0.30 V. The order of magnitude obtained for k_{et} was 10^5 s^{-1}, which corresponds to a heterogeneous pseudo-first-

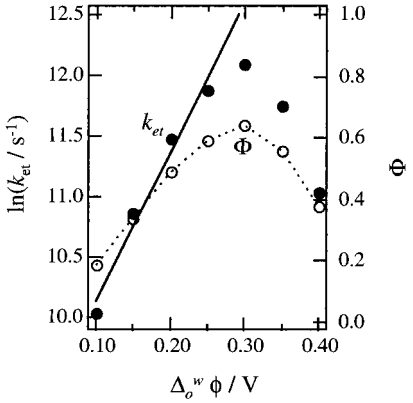

Figure 9. Electron-transfer rate constant (k_{et}) and quantum yield (Φ) as functions of the Galvani potential difference. A Butler−Volmer behavior is observed in the potential range around the pzc. The dashed line corresponds to an apparent transfer coefficient of 0.32. At potentials higher than 0.25 V, the ET kinetics is affected by the photoreaction involving $TPBCl^-$ (see text).

order rate constant of 10^{-2} cm s^{-1}, assuming a reaction layer of 1 nm.[38] It should be pointed out that these estimations are based on the measurement of the excited-state lifetime. As mentioned previously, k_d was obtained from flash photolysis in TIR at the water/DCE interface. However, this approach does not only monitored the adsorbed porphyrin but also the molecules located within the evanescent wave. This region extends a few hundreds of nanometers into the aqueous phase; therefore, there is some uncertainty on whether the adsorbed porphyrin exhibits a k_d of the order of 10^5 s^{-1}. In any case, the potential dependence of the photocurrent indicates unambiguously that k_{et} and k_d are of the same order of magnitude.

The quantum yield of the photoprocess (Φ) can be readily estimated from

$$\Phi = \frac{k_{et}}{k_{et} + k_d} \tag{13}$$

The potential dependence of Φ is also displayed in Figure 9. An increase from about 20% to 65% in the range 0.10−0.30 V is observed. A fundamentally important aspect derived from the dependence of k_{et} and consequently Φ is that both quantities effectively increase while the surface concentration of porphyrin decreases. These results indicate that the apparent electron-transfer rate constant involving neutral quenchers such as Fc is not determined by changes in the interfacial concentration of the porphyrin.

The potential dependence of k_{et} in Figure 9 does not exhibit a purely Butler−Volmer behavior. A strong curvature is observed from potentials above 0.20 V, reflecting a clear change in the ET kinetics. This change in kinetics is associated with the photoreaction involving the organic supporting electrolyte. As shown in Figure 3, the background photocurrent also becomes more evident at potentials higher than 0.20 V. The increase of the background photocurrent is linked to the interfacial accumulation of $TPBCl^-$. This phenomenon, as well as the effect of the specific adsorption of the porphyrin, can be rationalized from the interfacial capacitance−potential curves shown in Figure 7. According to the potential of minimum interfacial capacitance for porphyrin concentrations of 10^{-4} mol dm^{-3}, the accumulation of $TPBCl^-$ occurs at a potential higher than 0.22 V. This result precisely coincides with the onset of the background photocurrent shown in Figure 3. Correspondingly, the appearance of the negative photocurrent is linked to

the interfacial accumulation of $BTPPA^+$. These unexpected findings may open up the possibility of studying ion distribution in the organic phase as a function of the Galvani potential difference, providing that the ions show some redox activity.

As mentioned previously, the potential dependence of k_{et} associated with the photooxidation of ferrocene is not a direct consequence of changing the interfacial concentration of the reactants. In Figure 9, a Butler−Volmer behavior is observed at potentials less positive than 0.22 V. The apparent transfer coefficient (α_{app}) estimated close to the potential of zero charge is 0.32 ± 0.03. According to the model introduced by Girault and Schiffrin[39] for electron transfer at ITIES, the apparent transfer coefficient may also include the work terms associated with the precursor and successor complexes of the electron-transfer step. In light of the small fraction of the Galvani potential difference developed in the aqueous side (5%) and the fact that the electron donor in the organic side is neutral, it can be assumed that the work term regarding the electron-transfer precursor is not dependent on the applied potential. Consequently, the observed transfer coefficient reflects the change in the activation energy for electron transfer as a function of the applied potential. However, the complicated interfacial potential distribution introduces considerable difficulties in rationalizing the nature of this activation energy. For instance, it is clear that if the potential distribution across the interface is determined by the coverage of porphyrin, the parameter b in eq 12 will also be dependent on the applied potential. Furthermore, this analysis has not considered that interfacial ion association could also decrease the effective charge of the adsorbed species. Therefore, the understanding of the potential dependence of k_{et} and θ requires a more sophisticated description of the liquid/liquid junction, including specific adsorption as well as interfacial ion association effects.

5. Conclusions

The photocurrent responses associated with heterogeneous quenching of the porphyrin $ZnTPPC^{4-}$ mainly involved adsorbed species at the water/DCE contact surface. The porphyrin adsorption exhibits a Langmuir behavior, and the surface coverage depends on the applied potential. Assuming a net charge −4 for the adsorbed species, the potential dependence of the coverage suggests that only 5% of the Galvani potential difference is located in the aqueous side. Furthermore, the potential dependence of the surface excess charge suggests the formation of interfacial ion pairs between the porphyrin and the organic phase cation $BTPPA^+$.

The potential dependence of the photocurrent associated with the quenching by ferrocene indicates that the electron-transfer rate is comparable with the excited-state decay. It was estimated that the pseudo-first-order electron-transfer rate constant k_{et} is of the order of 10^5 s^{-1}, and it does increase as the potential is increased. At potentials away from the potential of minimum interfacial capacitance, electron-transfer processes involving the organic supporting electrolyte become evident. The effect of the supporting electrolyte modifies the dynamics of the photocurrent associated with neutral quenchers. A fundamental point arising from these results is that the activation energy of the electron transfer is dependent on the interfacial potential in the case of neutral quenchers. This result support the conclusions established by Tsionsky et al.[7,9] for the dark electron transfer between neutral zinc porphyrins and $Ru(CN)_6^{4-}$ at the water/benzene interface. However, these authors reported a transfer coefficient of 0.5, which is higher than our estimations in the region close to the pzc. On the other hand, the electron-transfer involving charged species such as $TPBCl^-$ and $BTPPA^+$ seems to be determined by changes in interfacial concentrations of the ionic species rather than in the activation energy. This behavior seems to be more consistent with the model introduced by Girault[14] and more recently by Schmickler,[38] although the potential distribution across the interface in the present case is expected to be substantially different than any previous theoretical description.

Finally, the attractive quantum yields obtained in this preliminary study may provide a novel perspective to solar energy conversion. Although the interfacial behavior of porphyrins requires further research, the inherent properties of ITIES allow a closer look at the fundamental aspects. From the structural point of view, these molecular interfaces are considerably better defined than interfaces involving thin films or nanoporous semiconducting films.[40−42] Solar cells based on porphyrin-sensitized nanoporous TiO_2 electrodes have already been tested, exhibiting a maximum quantum yield of about 40%.[43] These interfaces feature a higher surface concentration of porphyrin, optimizing the interfacial light absorption. However, the porous semiconducting films exhibits a large density of surface defects, which hinders the electron transport and introduces energy losses. In this respect, one of the major advantages of liquid/liquid junctions is that the conversion efficiency is determined by the properties of the sensitizer and quencher. For example, Fc exhibits a maximum Φ of about 60%, which can be increased to 90% upon replacing the quencher by DFcEt. Obviously, important aspects such as back electron transfer and excited-state diffusion are yet to be included in these preliminary estimations. Nevertheless, these initial steps reflect the versatility and potentiality of liquid/liquid interfaces for solar energy conversion.

Acknowledgment. We are grateful for the financial support of the Fonds National Suisse de la Recherche Scientifique (Project 2000-043381-95/1). We also acknowledge the contributions from Professor R. M. Corn, K. Kalyanasundaram, P. Galletto, S. Loridant, and L. Tomaszewski. We are also indebted to the technical assistance by Valérie Devaud. The Laboratoire d'Electrochimie is part of the European Network ODRELLI (Organization, Dynamics and Reactivity at Electrified Liquid/Liquid interfaces).

References and Notes

(1) Bard, A. J.; Cliffel, D. E.; Demaille, C.; Fan, F. R. F.; Tsionsky, M. *Ann. Chim.* **1997**, *87*, 15−31.

(2) Cheng, Y.; Schiffrin, D. J. *J. Chem. Soc., Faraday Trans.* **1993**, *89*, 199−205.

(3) Chen, Q. Z.; Iwamoto, K.; Seno, M. *Electrochim. Acta* **1991**, *36*, 291−6.

(4) Cheng, Y. F.; Cunnane, V. J.; Kontturi, A. K.; Kontturi, K.; Schiffrin, D. J. *J. Phys. Chem.* **1996**, *100*, 15470−15477.

(5) Ding, Z.; Fermin, D. J.; Brevet, P.-F.; Girault, H. H. *J. Electroanal. Chem.*, in press.

(6) Webster, R. D.; Dryfe, R. A. W.; Coles, B. A.; Compton, R. G. *Anal. Chem.* **1998**, *70*, 792−800.

(7) Tsionsky, M.; Bard, A. J.; Mirkin, M. V. *J. Phys. Chem.* **1996**, *100*, 17881−17888.

(8) Tsionsky, M.; Cardon, Z. G.; Bard, A. J.; Jackson, R. B. *Plant Physiol.* **1997**, *113*, 895−901.

(9) Tsionsky, M.; Bard, A. J.; Mirkin, M. V. *J. Am. Chem. Soc.* **1997**, *119*, 10785−10792.

(10) Kavarnos, G. J. *Fundamentals of photoinduced electron transfer*; VCH Publishers: New York, 1993.

(11) Gould, I. R.; Moser, J. E.; Armitage, B.; Farid, S. *Res. Chem. Intermed.* **1995**, *21*, 793.

(12) Brugger, P.-A.; Gratzel, M. *J. Am. Chem. Soc.* **1980**, *102*, 2461.

(13) Steiner, U. E.; Ulrich, T. *Chem. Rev.* **1989**, *89*, 51.

(14) Girault, H. H. In *Modern Aspects of Electrochemistry*; Bockris, J. O. M., Conway, B. E., White, R. E., Eds.; Plenum Press: New York, 1993; pp 1−62.
(15) Kotov, N. A.; Kuzmin, M. G. *J. Electroanal. Chem.* **1990**, *285*, 223.
(16) Kotov, N. A.; Kuzmin, M. G. *J. Electroanal. Chem.* **1992**, *341*, 47−60.
(17) Kotov, N. A.; Kuzmin, M. G. *J. Electroanal. Chem.* **1992**, *338*, 99.
(18) Hong, F. T.; Mauzerall, D. *J. Electrochem. Soc.* **1976**, *123*, 1317.
(19) Woodle, M. C.; Mauzerall, D. *Biophys. J.* **1986**, *50*, 431−439.
(20) Woodle, M. C.; Zhang, J. W.; Mauzerall, D. *Biophys. J.* **1987**, *52*, 577−586.
(21) Ilani, A.; Liu, T. M.; Mauzerall, D. *Biophys. J.* **1985**, *47*, 679−684.
(22) Hwang, K. C.; Mauzerall, D. *Nature* **1993**, *361*, 138−140.
(23) Brown, A. R.; Yellowlees, L. J.; Girault, H. H. *J. Chem. Soc., Faraday Trans.* **1993**, *89*, 207−12.
(24) Thomson, F. L.; Yellowlees, L. J.; Girault, H. H. *J. Chem. Soc., Chem. Commun.* **1988**, 1547−9.
(25) Marecek, V.; De Armond, A. H.; De Armond, M. K. *J. Am. Chem. Soc.* **1989**, *111*, 2561−4.
(26) Kott, K. L.; Higgins, D. A.; McMahon, R. J.; Corn, R. M. *J. Am. Chem. Soc.* **1993**, *115*, 5342−5343.
(27) Dryfe, R. A. W.; Ding, Z. F.; Wellington, R. G.; Brevet, P. F.; Kuznetzov, A. M.; Girault, H. H. *J. Phys. Chem. A* **1997**, *101*, 2519−2524.
(28) Duong, H. D.; Brevet, P. F.; Girault, H. H. *J. Photochem. Photobiol.* in press.
(29) Fermin, D. J.; Ding, Z.; Duong, H. D.; Brevet, P. F.; Girault, H. H. *Chem. Commun.* **1998**, *1125−1126*.
(30) Shao, Y. Ph.D. Thesis, University of Edinburgh, Edinburgh, 1991.
(31) Peter, L. M. *Chem. Rev.* **1990**, *90*, 753−769.
(32) Peter, L. M. In *Photocatalysis and Environment*; Schiavello, M., Eds.; Kluwer Academic Publishers: London, 1988; pp 243−273.
(33) Volkov, A. G. *Langmuir* **1996**, *12*, 3315−3319.
(34) Pereira, C. M.; Schmickler, W.; Silva, F.; Sousa, M. J. *J. Electroanal. Chem.* **1997**, *436*, 9−15.
(35) Cunnane, V. J.; Geblewicz, G.; Schiffrin, D. J. *Electrochim. Acta* **1995**, *40*, 3005−3014.
(36) Kalyanasundaram, K. *Photochemistry of Polypyridine and Porphyrin Complexes*; Academic Press: London, 1992.
(37) Higgins, D. A.; Corn, R. M. *J. Phys. Chem.* **1993**, *97*, 489−493.
(38) Schmickler, W. *J. Electroanal. Chem.* **1997**, *429*, 123−127.
(39) Girault, H. H. J.; Schiffrin, D. J. *J. Electroanal. Chem.* **1988**, *244*, 15−26.
(40) Bube, R. H. *Photoelectronic Properties of Semiconductors*; Cambridge University Press: Cambridge, 1992.
(41) O'Reagan, B.; Grätzel, M. *Nature* **1991**, *353*, 737.
(42) Grätzel, M. *Platinum Met. Rev.* **1994**, *38*, 151.
(43) Boschloo, G. Ph.D. Thesis, Delft University, Delft, 1996.